Chemosphere 302 (2022) 134909

Contents lists available at ScienceDirect

Chemosphere

journal homepage: www.elsevier.com/locate/chemosphere

Influence of dissolution on the uptake of bimetallic nanoparticles Au@Ag-NPs in soil organism *Eisenia fetida*

M. Baccaro [a,*], M.D. Montaño [b], X. Cui [c], A. Mackevica [b], I. Lynch [c], F. von der Kammer [b], R.W. Lodge [d], A.N. Khlobystov [d], N.W. van den Brink [a]

[a] Division of Toxicology, Wageningen University & Research, P.O. Box 8000, 6700, EA, Wageningen, the Netherlands
[b] Department of Environmental Geosciences, University of Vienna, 14 Althanstraße, Vienna, 1090, Austria
[c] School of Geography, Earth and Environmental Sciences, University of Birmingham, Edgbaston, Birmingham, B15 2TT, United Kingdom
[d] School of Chemistry, University of Nottingham, University Park, Nottingham, NG7 2RD, United Kingdom

HIGHLIGHTS

- Dissolution is the primary mechanism driving the uptake of metal NPs in earthworms.
- True bimetallic NPs represent only the 5% of the total concentration of metals in the earthworm.
- Transformation of the shell of bimetallic NPs occur in the earthworms.
- Ag and Au accumulation differs between earthworms exposed to one or both metals.

GRAPHICAL ABSTRACT

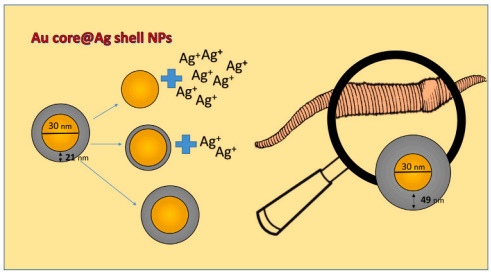

ARTICLE INFO

Handling Editor: Willie Peijnenburg

Keywords:
Accumulation
Bimetallic nanoparticle
Earthworm
Soil
Metal mixture

ABSTRACT

A key aspect in the safety testing of metal nanoparticles (NPs) is the measurement of their dissolution and of the true particle uptake in organisms. Here, based on the tendency of Ag-NP to dissolve and Au-NP to be inert in the environment, we exposed the earthworm *Eisenia fetida* to Au core-Ag shell NPs (Au@Ag-NPs, Ag-NPs with a Au core) and to both single and combined exposures of non-coated Au-NPs, Ag-NPs, Ag^{+} and Au^{+} ions in natural soil. Our hypothesis was that the Ag shell would partially or completely dissolve from the Au@Ag-NPs and that the Au core would thereby behave as a tracer of particulate uptake. Au and Ag concentrations were quantified in all the soils, in soil extract and in organisms by inductively coupled plasma mass spectrometry (ICP-MS). The earthworm exposed to Au@Ag-NPs, and to all the combinations of Ag and Au, were analyzed by single particle inductively coupled plasma time-of-flight mass spectrometry (spICP-TOFMS) to allow the quantification of the metals that were truly part of a bimetallic particle. Results showed that only 5% of the total metal amounts in the earthworm were in the bimetallic particulate form and that the Ag shell increased in thickness, suggesting that biotransformation processes took place at the surface of the NPs. Additionally, the co-exposure to both metal ions led to a different uptake pattern compared to the single metal exposures. The study unequivocally confirmed that dissolution is the primary mechanism driving the uptake of (dissolving) metal NPs in earthworms. Therefore, the assessment of the uptake of metal nanoparticles is conservatively covered by the assessment of the uptake of their ionic counterpart.

* Corresponding author.
E-mail address: marta.baccaro@wur.nl (M. Baccaro).

https://doi.org/10.1016/j.chemosphere.2022.134909
Received 17 March 2022; Received in revised form 6 May 2022; Accepted 7 May 2022
Available online 10 May 2022

1. Introduction

Assessing the true bioaccumulative potential of metal nanoparticles (NPs) is challenged by difficulties in discriminating the uptake of true NPs from the ionic counterparts that may be more available to an organism. Ions, including those released from metallic NPs, are considered to be more bioavailable than the particulate form, and therefore more easily taken up in organisms (Savoly et al., 2016; Laycock et al., 2017; Baccaro et al., 2018; Noventa et al., 2018). In soil, the main driver of metal NP bioavailability is attributed to dissolution processes. In studies utilising different metal NPs, significant relationships between concentrations of ionic metals in soil pore water and metal accumulation in soil organisms have been reported (Laycock et al., 2017; Bollyn et al., 2018). However, it was not possible to completely exclude or quantify the uptake of metals in their particulate form. This is exemplified by studies reporting the uptake of supposably non-dissolving Ag_2S-NPs in isopods (Kampe et al., 2018) and in earthworms (Baccaro et al., 2018). However, in a previous study little uptake of Ag was detected in earthworms exposed to Ag_2S-NPs indicating that the Ag_2S-NP were only partially sulfidized which could have led to a partial release of ions, driving the uptake in earthworms (Baccaro et al., 2018). Nevertheless, when modelling the uptake of Ag_2S-NPs, and considering only dissolved Ag concentrations as the exposure concentrations (extremely low), the ionic uptake was unable to justify the entire uptake found with the Ag_2S-NPs, suggesting that uptake of particulate Ag could take place (van den Brink et al., 2019).

Whilst the bioavailability of NP is reduced due to binding and retention of metal NPs in the solid matrix (Cornelis et al., 2014; Tavares et al., 2015), this fraction can still be available for organisms that ingest soil particles, like earthworms (Lanno et al., 2004). Therefore the concentrations of the metal from non-dissolving (insoluble) NPs available in the soil pore water may not fully explain their accumulation in the earthworm. Indeed, the dietary uptake of metals and metal NPs was shown to be the primary route of exposure that should be considered when assessing bioavailability (Vijver et al., 2003; Diez Ortiz et al., 2015).

In order to investigate whether dissolution is the primary process for the uptake of dissolving metal NPs in earthworms in natural soils, we performed a bioaccumulation test using bimetallic NPs, composed of an Au core surrounded by an Ag shell (Au@Ag-NPs, Ag-NPs with a Au core) and combined exposure of Au-NPs, Ag-NPs, Ag and Au ions in all combinations. The Au core of the bimetallic NPs was not expected to dissolve over the time course of the 4 week exposure and could therefore be used as a nano-tracer, while the outer shell made of Ag would interact with the exposure media and dissolve. Comparing accumulated Ag and Au from the different particle/ionic forms provided information about how dissolution affected the uptake of the different forms by the earthworm. Additionally, ethylene-diaminetetraacetic acid (EDTA) soil extractions were performed to quantify the bio-accessible Au and Ag fractions in the soil in the different exposure scenarios (Lo and Yang, 1999). Based on the results, the roles of particulate versus ionic forms in the accumulation of metal NPs into earthworms was critically scrutinized.

2. Materials and methods

2.1. Nanoparticle synthesis and characterization

2.1.1. Synthesis of 50 nm Ag-NPs

Ag-NPs (50 nm) were synthesized and characterized by Applied Nanoparticles (Barcelona, Spain) as already reported in Baccaro et al. (2018). Briefly, an aqueous solution (100 mL) containing trisodium citrate (SC, 5 mM) and tannic acid (TA, 0.25 μM) was prepared and heated using a heating mantle in a three-neck round-bottomed flask for 15 min under vigorous stirring. After boiling had commenced, $AgNO_3$ (1 mL of 25 mM) was injected into this solution. The solution became bright yellow. Immediately after the synthesis of the Ag seeds and in the same vessel, the solution was diluted by extracting 19.5 mL of sample and adding 16.5 mL of MilliQ water. Then, the temperature of the solution was set to 90 °C and 500 μL of SC (25 mM), 1.5 mL of TA (2.5 mM), and 1 mL of $AgNO_3$ were sequentially injected (time delay ~ 1 min). Aliquots were purified by centrifugation (10000 g) in order to remove the excess of TA and further redispersed in SC 2.2 mM.

2.1.2. Synthesis of 13 nm Au-NPs seeds

Au-NP seeds were synthesized following a published protocol with minor modifications (Kumar et al., 2007). Typically, $HAuCl_4$ solution (5 mL of 28.8 mmol L^{-1}) was diluted to 150 mL with ultrapure water and heated using a metal bath with temperature set at 105 °C. Upon quick injection of sodium citrate solution (15 mL of 38.8 mmol L^{-1}) under reflux and stirring, the yellow solution became colourless within 2 min, turning black and finally red colour. The system was kept at 105 °C for 50 min and then cooled to room temperature. The resultant solution was kept at 4 °C without further purification for future characterization and synthesis of larger Au-NPs and Au@Ag-NPs.

2.1.3. Synthesis of 30 nm Au-NPs

To a flask containing ultrapure water (340 mL), Au-NPs solution (50 mL of 13 nm seeds) and hydroxylamine (10 mL of 4 mmol L^{-1}) was added. $HAuCl_4$ solution (100 mL of 1.62 mmol L^{-1}) was dropwise added into the NP solution under stirring. Once the addition of $HAuCl_4$ solution had finished, sodium citrate solution (15 mL of 38.8 mmol L^{-1}) was added as the stabilizing agent. The resultant NP solution was kept at 4 °C without purification for future characterization and usage.

2.1.4. Synthesis of 60 nm Au@Ag NPs

13 nm Au-NP (50 mL) seed solution was diluted with ultrapure water (50 mL), and ascorbic acid (2 mmol) was added under stirring. Upon dropwise addition of a $AgNO_3$ solution (100 mL of 10 mmol L^{-1}) under stirring at 50 °C, the red solution gradually became browner in colour over 5 min. After the addition of the $AgNO_3$ solution polyvinylpyrrolidone (PVP) (200 mg, molecular weight 40,000) was added under stirring. The system was maintained at 50 °C for another 10 min. The resultant core-shell NP solution was kept at 4 °C without purification for future characterization and usage. The mass concentration of Au core-Ag shell NPs was determined by ICP-MS following acid digestion in *aqua regia* (1 : 3 nitric acid: hydrochloric acid) and was determined to be 498.3 ± 57.7 μg mL^{-1} for Ag and 24.9 ± 1.9 μg mL^{-1} for Au, respectively.

2.1.5. Electron microscopy analysis

Holey carbon film on copper mesh TEM grids were purchased from Agar Scientific Ltd., UK. TEM analysis was performed on a JEOL 2100F FEG-TEM with accelerating voltages of 80 kV and 200 kV (field emission electron gun source, information limit 0.19 nm). Images were acquired using Gatan Digital Micrograph. EDX spectroscopy was performed using an Oxford Instruments XMax 80 T silicon drift detector with INCA Energy 250 Microanalysis system.

2.2. Earthworm culturing

The earthworm *Eisenia fetida* is a model organism extensively used in standardized ecotoxicological tests. *E. fetida* were supplied by Lasebo (Nijkerkerveen, The Netherlands) and kept in the same soil used for the experiments in an incubator at 20 ± 1 °C with 24 h of light for approximately 2 weeks prior to the experiments and were fed with horse manure from an organic farm (Bennekom, The Netherlands) with known absence of pharmaceutical use.

2.3. Soil preparation and exposure

Earthworms were exposed in natural soil (pH 5.98 in water, organic matter content 5.4%) collected from an organic farm in The Netherlands

(Proefboerderij Kooijenburg, Marwijksoord, Netherlands), air dried and sifted (5 mm sieve openings) before use. Glass jars with a lid were prepared with air dried soil (450 g) with additional water (20% w/w, ~47% water holding capacity). Soils were spiked with Au@Ag-NPs, Ag-NPs, Au-NPs, $AgNO_3$, $HAuCl_4$ to reach a nominal concentration of 25 mg Ag kg^{-1} and 1.5 mg Au kg^{-1} for all treatments (for actual soil concentrations see Fig. 5). The ratio between nominal Ag/Au concentrations spiked into the soils were as per the nominal concentrations of Au and Ag in the Au@Ag-NPs dispersion (500 μg Ag mL^{-1} and 30 μg Au mL^{-1}). Soil, water and metal(s) solutions were homogeneously mixed by an automatic mixer for 3 min and jars were filled. After 24 h, 8 adult *E. fetida* earthworms with an average weight of 478.31 ± 44 mg (n = 360) per earthworm were randomly placed into every experimental unit. Although in the case of soil spiked with metal salts, an equilibration time of 7 days is usually used, in order to perform a comparison between uptake in earthworms after combined exposure to metal salt and metal particles, the duration of the soil aging has been set the same across the treatments (24 h).

2.4. Sampling

After 28 days, jars were separately emptied. Aliquots of soil were sampled and stored at −20 °C. Worms were collected, carefully rinsed with deionized water, dried in a double layer of tissue paper and placed in glass Petri dishes to depurate in the incubator at 20 °C for 24 h. After depuration, worms were rinsed again with deionized water and dried. Worms from each jar were pooled and snap frozen in liquid nitrogen and stored at −80 °C for further analysis.

2.5. EDTA extraction of soil

Soil (1 g) was mixed with disodium EDTA (10 mL, 0.05 M) at pH 7.0 and overhead shaken overnight (~18 h). The slurry was filtered through preconditioned (soaked in a solution $CuNO_3$ (0.1 M, 99.9%, Sigma Aldrich) overnight before use) 0.45 μm filters and directly acid digested for Ag and Au quantification.

2.6. Extraction and analysis of total Ag and Au

The extraction of total Ag and Au from soil, worm tissues and EDTA soil extracts was performed by microwave assisted (MARS 6, microwave system, CEM Corporation) acid digestion in *aqua regia* (1 : 3 nitric acid–hydrochloric acid). Aliquots of samples were weighed (~0.5 g of wet soil, worm tissue or 2.5 mL of soil EDTA extract) and placed in Teflon vessels with 6 mL of HCl 37% (Merck, Darmstadt) and 2 mL of HNO_3 69% (Merck, Darmstadt). A two temperature steps programme was used (ramp to 160 °C in 10 min, 30 min hold, ramp to 200 °C in 10 min and 30 min hold). Samples were analyzed for total Au and Ag, using ICP-MS Nexion 350D (PerkinElmer Inc., Waltham, MA). The metals quantified were Ag (*m/z* 107 and 109), Au (*m/z* 197) and Rh (*m/z* 103) as internal standard. Calibration curves were prepared from standards of Ag^+ and Au^+ (standard stock solution 1000 mg L^{-1} Ag, Merck, Darmstadt). The limit of detection (LOD) of Ag (*m/z* 107) and Au was calculated as the mean of digested blank + 3σ blank, and found to be 0.5 μg L^{-1}.

2.7. Extraction and particulate analysis of bimetallic nanoparticles

Bimetallic Au@Ag-NPs were extracted from the earthworms' tissue by incubation of finely ground worm tissue (~425 ± 22 mg (n = 5)) in alkaline solution (8 mL, tetramethylammonium hydroxide (TMAH) 20%) overnight (Gray et al., 2013). The samples were diluted 1000x prior to analysis by single particle Inductively Coupled Plasma Time of Flight Mass Spectrometry (spICP-TOFMS, icpTOF 2R, TOFWERK AG, Switzerland). This instrument recorded a broad swatch of the atomic mass spectrum (7–250 *m/z*) at 46 μs intervals, permitting the *quasi*-simultaneous detection of multiple elements on a particle-by-particle basis. The principles of spICP-MS are described elsewhere (Pace et al., 2011; Montano et al., 2016). Briefly, a known particle size standard is used to determine the transport efficiency, which is then used to calculate a mass flux calibration slope. This calibration curve slope is then used to relate the ion signal intensity to mass, which is subsequently converted into diameter assuming a specific geometry and density (see formulas in paragraph S6). The dissolved metal curves used to relate the signal to the mass were prepared in trace metal grade nitric acid. Transport efficiency was calculated using well-characterized 100 nm gold NPs (BBI solutions) resulting in a transport efficiency of 6.43%. The dwell time was set at 3 ms and data on mass, volume and size were selected in order to only process the intensity signals when Au and at least one Ag isotope (Ag 107 or Ag 109) were detected. Particle events were detected using a modified method adopted from Pace et al. (2011). Here particles events are described as those signal intensities which exceed a threshold set by the iterative application of a μ+3σ cut-off (where μ is the average of all intensities and σ is the standard deviation).

2.8. Data processing and statistics

The data acquired from spICP-TOFMS were further processed in Microsoft Excel. Post hoc Tukey multiple comparison test following one way ANOVA and Welch multiple correction test following *t*-test were performed by GraphPad Prism version 7.

3. Results

3.1. Nanomaterials characterization

A transmission electron microscopy (TEM) was used to study the size, morphology and structure of the NPs. TEM showed that the Ag-NPs and Au-NPs were spherical shaped particles with size equal to 50.0 ± 7.4 nm (minor axis± SD, N = 371) and 33.1 ± 5.8 nm (minor axis± SD, N = 1110), respectively (Fig. 1a–b). *Quasi*-spherical Au@Ag were achieved *via* a seeded approach by using 13.1 ± 2.6 nm (minor axis ±SD, N = 463) Au NPs as seeds. The size increase to 54.1 ± 16.7 nm (minor axis ± SD, N = 298) after coating of the Au seeds with a Ag layer (Fig. 1c). Size distributions are reported in Figure S1. In addition to the increase in particle size, the core-shell structure of Au@Ag-NPs was further confirmed by high angle annular dark field (HAADF) imaging and element mapping by EDX spectroscopy (Figs. 2 and 3). As observed by the HAADF image in Fig. 4, some particles consisted of more than one Au core inside an Ag shell, which are spots with higher contrast compared to the Ag shell. The size increase of the Au-NPs was reflected by a blue shift on their surface plasmonic absorbance on UV–vis. Likewise, after coating with an Ag layer, a significant shift of absorbance maximum, from 525 nm to 450 nm, was observed (Figure S2). The equivalent size of the Au core detected by spICP-TOFMS was larger than the size of Au seed NPs, ~30 nm *vs* ~13 nm, which is likely attributed to the fact that some core-shell NPs consist of multiple Au cores (Fig. 3). Larger agglomerates in the Au@Ag-NPs stock solution were removed by an ultrafiltration. Only negligible amounts of the ionic form of Ag or Au were detected in the ultrafiltrate by ICP-MS (paragraph S5). Additional characterization data of the Ag-NPs and Au-NPs are reported in the supplemental information, in Figures S1 and S2.

3.2. Exposure characterization

Actual Ag and Au concentrations in soil (mg metal kg^{-1} soil, wet weight) were measured in each replicate following acid digestion by *aqua regia* (graphical representation in Fig. 5, numerical concentrations in Table S1) resulting in average recoveries of 88 ± 8% and 107 ± 16% of the nominal concentrations (25 mg Ag kg^{-1} and 1.5 mg Au kg^{-1}) for Ag and Au, respectively. Ag and Au were also quantified in soil extracted

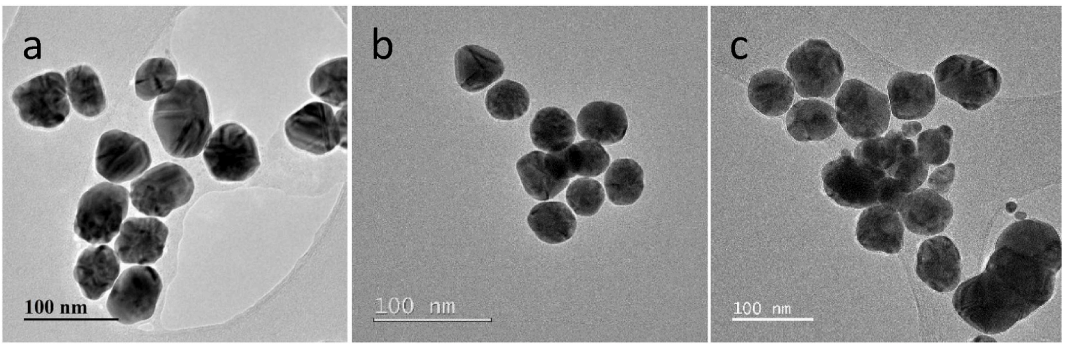

Fig. 1. TEM images of a) Ag-NPs, b) Au-NPs, c) Au@Ag-NPs

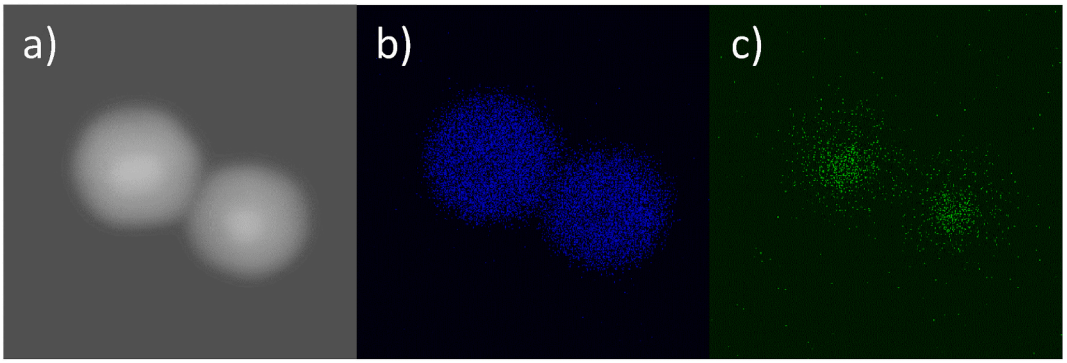

Fig. 2. a) HAADF images of Au@Ag-NPs and EDS elemental mapping of b) silver and c) gold distribution in Au@Ag-NPs. (For interpretation of the references to colour in this figure legend, the reader is referred to the Web version of this article.)

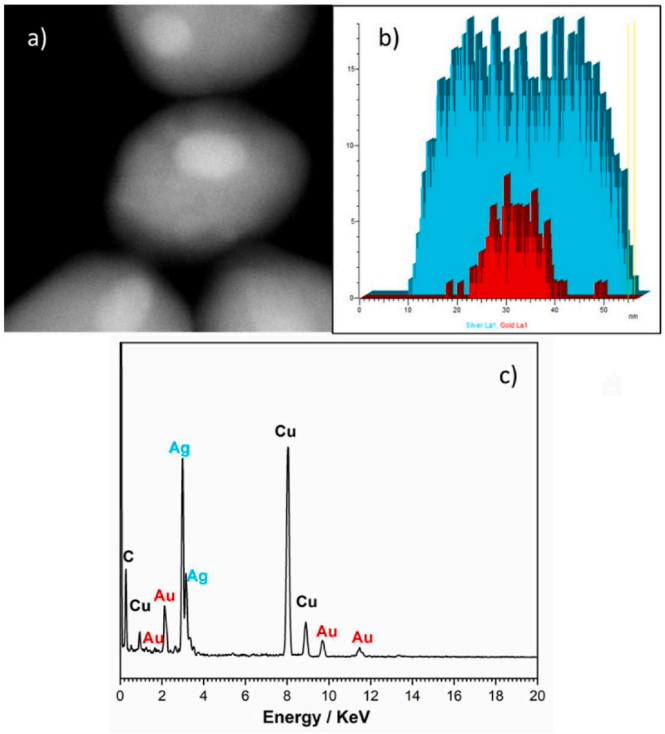

Fig. 3. a) HAADF of a Au@Ag-NP, b) EDX line spectra (light blue corresponds to the element Ag, the red colour corresponds to the element Au) and c) EDX spectrum of the same particle (Cu peak is due to the TEM sample holder). (For interpretation of the references to colour in this figure legend, the reader is referred to the Web version of this article.)

by EDTA (graphical representation in Fig. 6, numerical concentrations in Table S2). Variable concentrations denoted statistical differences. Results of statistical analysis (test *post hoc* Tukey multiple comparison test following one-way ANOVA) are reported in Table S2.

3.3. Bioaccumulation in the earthworms

The accumulation of Ag and Au in earthworms exposed to the different treatments is presented in Fig. 7. Numerical concentrations (average ± standard deviation, n = 5) are reported in Table S3. No internal Ag concentration resulted to be statistically different between worms exposed to the different forms of Ag. In the case of Au, the single ionic Au exposure led to an Au uptake which was statistically higher than all the combined exposures (Au^{+} + Ag^{+}, AuNP + Ag-NP, Ag-NP + Au^{+}, Ag^{+} + Au-NP) (Table S3). Uptake of ionic Au in co-exposure with different forms of Ag (i.e., ionic versus particulate) differed significantly, depending on the Ag form (Table S3). Background Ag concentration in earthworms from the same population was quantified in our previous study and was determined to be 0.04 ± 0.01 mg Ag/kg wet body weight (n = 24; mean ± standard deviation). Background Au concentrations in earthworms have been reported as lower than 0.003 mg Au/kg wet body weight (n = 8) (Bourdineaud et al., 2019).

The organisms exposed to any combination of Ag and Au in both ionic or particulate form were also analyzed by spICP-TOFMS for multi-element detection of bimetallic NPs (Naasz et al., 2018). Table 1 reports the mass concentrations and thickness of the shell and diameter of the core of the bimetallic NPs detected in the stock solution and in the earthworms. Au and Ag concentrations in the bimetallic NPs detected in the earthworms were both statistically different from the control only in the case of Au@Ag-NP and Ag-NP + Au^{+} exposure (Table S4). In paragraph S6, the formulas used for the calculation of the volume of the shell and particle mass concentrations are presented.

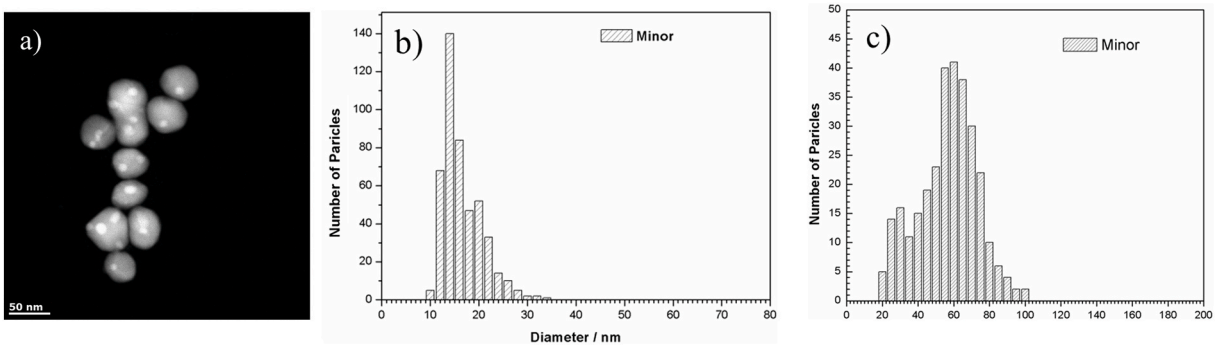

Fig. 4. a) HAADF image of Au@Ag-NPs where double/multiple Au cores were visible as higher contrast areas within the particles, b) size distribution (minor axes± SD, 13.1 ± 2.6 nm, N = 463) of Au core and c) of Au@Ag-NPs as Au–Ag structure (minor axis± SD, 54.1 ± 16.7, N = 298).

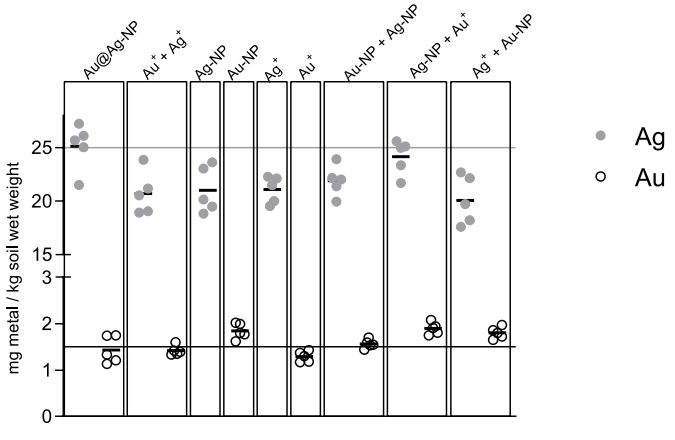

Fig. 5. Total Ag and Au exposure concentrations (n = 5) in spiked soil measured by ICP-MS following acid digestion (mg/kg wet weight). Solid horizontal lines represent the intended nominal concentration for Ag (grey line) and Au (black line). Solid marks indicate average concentrations for the treatment.

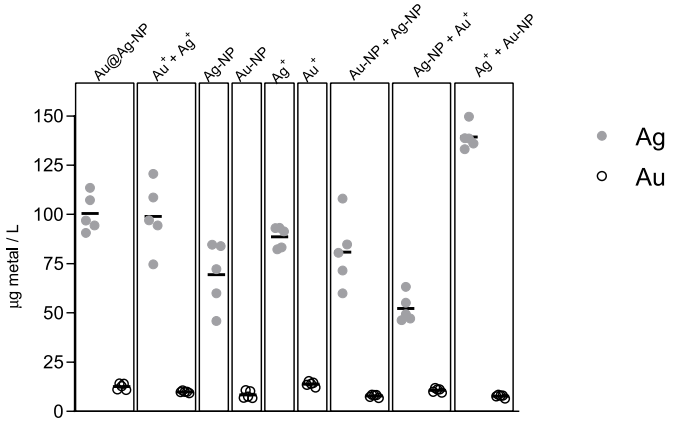

Fig. 6. Total Ag and Au concentrations (n = 5) in EDTA soil extracts measured by ICP-MS following acid digestion (µg/L).

4. Discussion

4.1. Exposure characterization

Regardless of the form in which Ag was added to the soil, total Ag uptake in earthworms, measured by ICP-MS, was not significantly different amongst Ag treatments. This supports the hypothesis that Ag from the shell of the bimetallic NPs (Au@Ag-NPs) dissolved and that the

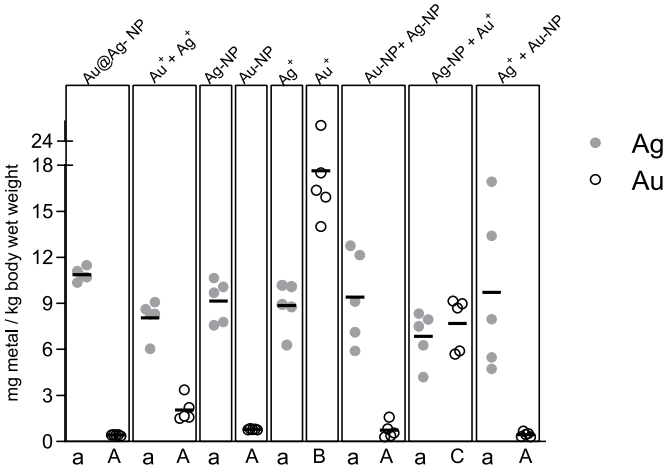

Fig. 7. Total Ag and Au concentrations in earthworm tissue after 28 days exposure measured by ICP-MS following acid digestion. Average values with the same letters are not significantly different (*post hoc* Tukey multiple comparison test following one-way ANOVA).

released Ag ions were taken up by the earthworms in a similar way compared to ions released from Ag-NPs and to ionic Ag from $AgNO_3$. The same process has been discussed using a kinetic model in our previous work (Baccaro et al., 2018).

The comparison amongst the concentrations of Au in earthworms exposed to all the combined treatments highlights statistically significant differences. Although the concentrations in earthworms exposed to particulate Au (Au@Ag-NPs and Au-NPs) do not show statistically significant differences from one another and are <1 mg Au kg^{-1}, when the exposure includes only ionic Au, the concentration in the earthworms reaches 17.6 ± 4.0 mg Au kg^{-1}. To the authors knowledge, the only study that assessed the bioavailability and uptake of Au and Au-NPs in earthworms is the work of Unrine et al. (2010) who also reported that *E. fetida* exposed to $HAuCl_4$ and Au-NPs accumulated both ionic Au and nano Au but that the ionic form was taken up to a larger extent. However, in the current study when earthworms are exposed to Au^+ in the presence of either form of Ag (Au^+ vs Au-NP + Ag-NP; Au^+ vs Ag-NP + Au^+; Au^+ vs Ag^+ + Au-NP) the internal Au concentrations are significantly lower than when earthworms are only exposed to Au^+ (Fig. 7) suggesting a potential interaction between the two elements in the soil. The nucleation of bimetallic Ag–Au nanocrystals from the interactions between Ag^+ and Au^+ and fulvic and humic acids has been previously reported (Alivio et al., 2018; Sharma et al., 2019). In the present study, it is hypothesized that the complexation of Ag^+ and Au^+ with soil components may have occurred and decreased the amount of free and available ions, especially Au^+, to earthworms. Au concentrations in

Table 1
Concentrations (as bimetallic NPs) and thickness of shell and diameter of core of the bimetallic NPs detected in the stock solution (n = 3) and in earthworm tissue samples (n = 5) exposed to Au@Ag-NPs and different combination of Ag and Au in both ionic and particulate forms. Asterisks show statistically significant difference with the concentrations in the control.

	Mass Ag (mg kg^{-1})	Mass Au (mg kg^{-1})	Element shell	Element core	Thickness shell (nm)	Diameter core (nm)
Stock solution Au@Ag-NP	289.6 ± 2.8	26.5 ± 0.3	Ag	Au	21.7 ± 1.0	30.9 ± 0.2
Earthworm Au@Ag-NP	0.69 ± 0.4*	0.02 ± 0.01*	Ag	Au	49.3 ± 3.3	31.4 ± 0.9
Earthworm Ag-NP + Au^+	0.20 ± 0.08*	0.17 ± 0.10*	Au	Ag	6.3 ± 1.7	81.9 ± 5.7
Earthworm Au-NP + Ag^+	<0.001	0.004 ± 0.009	n.a.	n.a.	n.a.	n.a.
Earthworm Ag-NP + Au-NP	0.003 ± 0.002*	0.006 ± 0.010	n.a.	n.a.	n.a.	n.a.
Earthworm Ag^+ + Au^+	0.004 ± 0.001	0.001 ± 0.002	n.a.	n.a.	n.a.	n.a.
Earthworm Control	0.001 ± 0.001	0.001 ± 0.002	n.a.	n.a.	n.a.	n.a.

earthworms exposed to combined Au^+ + Ag^+ in the soils were significantly lower than in the earthworms exposed to Ag-NPs + Au^+, likely due to that fact that the Ag^+ in the Ag^+ exposures directly interacted with the Au ions, while in the Au^+ + Ag-NP exposure the Ag first needs to dissolve before it could interact with the Au ions. This permitted relatively efficient Au^+ accumulation by the worms. The effect of the Ag^+ + Au^+ complexation on bioavailability (lower uptake of Ag when co-exposed with Au) cannot be detected in the case of Ag (not significant differences between Ag from Ag^+ + Au^+ and Ag from Ag-NPs + Au^+) likely due to the excess of free Ag^+ compared to Au^+ (25 mg Ag kg^{-1} vs 1.5 mg Au kg^{-1}). Another explanation could be the competition among cations at the site of uptake. It was most likely that both ion complexation to the soil and cation competition play a role in the different uptakes of Ag and Au (Ardestani et al., 2015).

Since dissolution of metals in *aqua regia* is not representative of their bioavailable fraction, we extract the metals from the soil of each experimental jar using the chelating agent EDTA which has been studied as a chemical extractant useful for obtaining information on the phytoavailable metal fraction in soils (Chang et al., 2014). EDTA is known to be able to displace metals as well as carbonate-bound and organometallic complexes, which may represent the available fraction to soil-feeding organisms (Ernst, W.H.O., 1996; Bakircioglu et al., 2011). However, the concentrations of Ag and Au in the EDTA extractions showed variable results, suggesting that EDTA alone cannot linearly describe the fraction of Ag and Au that is bio-accessible by earthworms, likely because EDTA extracts do not take into account bioavailability via ingested soil particles within the gut. Pearson r coefficients are equal to 0.22 (n = 35, R^2 = 0.04, p = 0.228) and 0.64 (n = 35, R^2 = 0.30, p < 0.001) for Ag and Au, respectively (Fig. 8). Au concentrations in worms show a significant correlation with Au concentrations in the EDTA soil extracts, but this outcome does not match the results in the exposure to Au^+ only or Ag-NPs + Au^+. In these treatments (Au^+ only or Ag-NPs + Au^+), the Au concentration in earthworms is higher than in all the other Au treatments and this difference is not reflected as higher Au concentration in EDTA extracts. This difference could be the result of the binding affinity of Au to the soil particles.

4.2. Bioaccumulation in the earthworms: result of interactions between metal species

The quantification of bimetallic NPs by spICP-TOFMS highlights that 5.2% and 4.0% of the Ag and Au (based on total quantifications) taken up by the earthworms exposed to Au@Ag-NP are present as bimetallic NPs. Similarly, in our previous study (Baccaro et al., 2018) we reported that around 15% of the Ag determined to be present in earthworms exposed to Ag-NPs were present in the particulate form (measured by spICP-MS). As reported in the paragraph 3.3, bimetallic NPs were also quantified in the earthworms exposed to Ag-NP + Au^+. Biogenic formation of Ag-NPs occurs in organisms exposed to Ag ions (Baccaro et al., 2018). In a similar way particulate Ag and Au could behave as nucleation bodies on which layers of dissolved metal can deposit to form a shell. However, this process is dependent on the internalized concentration (Mohsin et al., 2020) and this is shown by the fact that bimetallic NPs are quantified to a significant extent only in the earthworms exposed to Ag-NP and Au^+ (2.5% and 2.6% of the total internalized Ag and Au, respectively). Indeed, only in this combined exposure condition earthworms accumulated Au as much as Ag (6.9 ± 1.7 and 7.7 ± 1.7 mg metal kg wet body $weight^{-1}$ for Ag and Au, respectively). With exposure to Ag^+ + Au^+, the internalized Au concentration was hampered and lower than the internalized Ag concentrations (8.1 ± 1.2 and 2.1 ± 0.8 mg metal kg wet body $weight^{-1}$ for Ag and Au, respectively), and thus the biogenic formation of bimetallic NPs was not occurring at a measurable level. However, the biogenic formation of Ag-NP cannot be excluded. Bimetallic NPs concentrations in the earthworms exposed to Au-NP + Ag^+, Ag-NP + Au-NP or Ag^+ + Au^+ were not significantly different than the values in control samples. In the same samples, the Au concentrations were always much lower than the Ag concentrations (4–25 times lower) and this therefore decreased the probability of interaction of the two metals.

However, the detection of particles with size below 20 nm is challenged against a high background of dissolved silver ions. This could lead to an underestimation of the concentration of bimetallic NPs in the earthworms, although the recovery of Au in the stock solution as

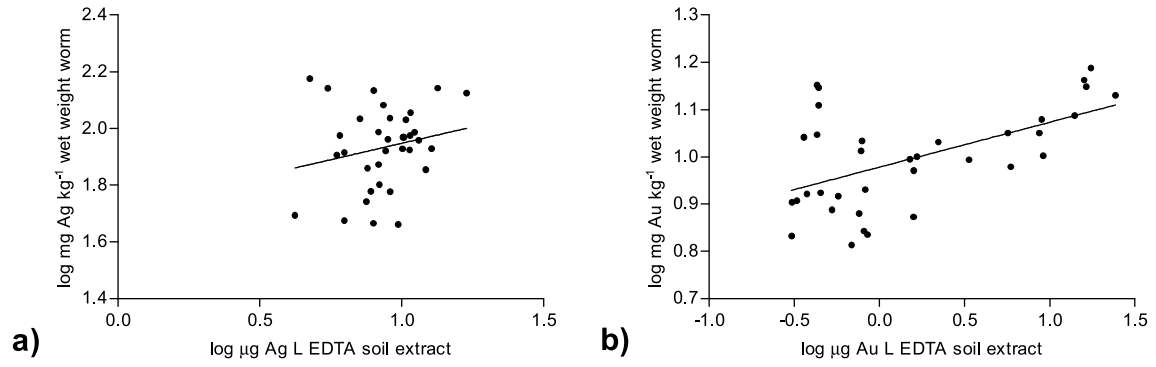

Fig. 8. Plot of log transformed Ag (a) and Au (b) concentrations in the earthworms as a function of log transformed Ag and Au concentrations in the EDTA soil extracts.

quantified by spICP-TOFMS is equal to 106% (24.9 ± 1.9 μg mL^{-1} by ICP-MS vs 26.5 ± 0.3 μg mL^{-1} by ICP-TOFMS). From the size distribution of the Au core particles in the stock, it can be calculated that 75% of the particles had sizes lower than 20 nm (TEM size distribution, Fig. 4b). In the worst case, in which just 25% of the Au-NPs were detected, this would lead to an estimated true gold particulate uptake of 0.08 mg Au kg^{-1} instead of 0.02 mg Au kg^{-1} in the earthworms exposed to Au@Ag-NPs. By calculating the Ag needed to have a shell of 22 nm around a 13 nm gold core (median value of the size distribution), the Ag belonging to a bimetallic NP would be 3.19 mg Ag kg^{-1} which represented 29% of the total Ag taken up in the earthworm. Nevertheless, as already mentioned above, the mass Au recovery by spICP-TOFMS was calculated to be 106% (Table 1) and for this reason we propose that it is more likely that the detected Au@Ag-NPs had multiple Au cores (Fig. 4) and that the spICP-TOFMS detected this as single Au core of ~30 nm.

Comparison of the bimetallic NP sizes within the earthworms exposed to Au@Ag-NPs and in the stock solution detected by the same analytical techniques, i.e., spICP-TOFMS (Table 1), suggested that the shell underwent some transformations because the Au core size in both cases (before and after uptake) remained unchanged as ~30 nm and the thickness of the Ag shell increased ~28 nm. The fact that Au core size did not change after uptake indicated that Au did not interact with the media. The increasing shell thickness would suggest that agglomeration processes may have occurred on the surface of the shell instead. The quantification of the exact increase was not possible due to a too broad size distribution of the initial Au@Ag-NPs stock solution (Fig. 4c). Merrifield et al. also used Au@Ag-NPs to study the transformations of Ag-NPs in complex media, and the NP size was monitored in hard water with the addition of fulvic acid (Merrifield et al., 2017). At similar concentrations to the concentrations measured after EDTA extraction in the present study (>1 μg L^{-1}) they reported an increase in the Ag shell thickness but not in the Au core size. The authors considered two possible scenarios. The organic matter formed a corona at the NPs surface and that Ag bound afterwards, causing a surface growth in the exposure media; or that Ag ions were aggregating on the surface of the Au@Ag-NP after they were taken up within the organism. The formation of the biocorona has been reported *in vivo* and *in vitro* (Lundqvist et al., 2008; Hayashi et al., 2013; Akter et al., 2018; Garcia-Alvarez et al., 2018). Soft and hard coronas have been reported to trap Ag ions and to form Ag_2S on the surface of the Ag-NP (Miclaus et al., 2016). Ag ions could originate from the NP itself or be located in the medium. If this mechanism takes place, spICP-TOFMS would still detect that particle as a bimetallic NP with a larger Ag shell compared to the original one. We propose that 5% of the detected internalized bimetallic NPs underwent a similar process resulting in the Ag shell becoming thicker (~+28 nm). We exclude any effect caused by the method used to extract the NPs from the earthworm tissue. Dong et al. (2018) showed that the sizes of Ag-NPs extracted by alkaline solution from the tissues were nearly identical to those in H_2O, suggesting that the Au-NP core was also stable in alkaline extracted tissue and retained its original size (core diameter) (Arslan et al., 2011; Gray et al., 2013; Loeschner et al., 2014).

Similar process may have occurred in earthworms exposed to Ag-NP and Au^+. Internalized Ag-NP increased their size due to aggregation of Ag ions on their surface, probably together with the formation of a biocorona (with shell thickness increasing from ~50 nm to ~80 nm). However, in this case Au ions would also take part in the layered structure, possibly as Au/Ag alloy layer (Mondal et al., 2011). This is then reflected in the spICP-TOFMS measurements that showed the presence of bimetallic NPs having a silver core and a gold shell (the opposite of the synthetic particles, which allowed clear differentiation of the original versus the biogenically produced NPs) (Table 1).

5. Conclusion

The quantification of Ag and Au in earthworms exposed to bimetallic NPs and different combination of nano- and ionic forms of Au and Ag unequivocally confirmed that dissolution was a driving factor for the uptake of metal NPs in earthworms. The accumulation of particulate metals from Ag-NPs with a Au core (Au@Ag-NPs) represented only 5% of the total amount of metals accumulated within the earthworm. Additionally, those bimetallic NPs were shown to be biotransformed having an unvaried size of the Au core and but a thickening of the Ag shell. Biogenic formation of bimetallic NPs was also reported, although interestingly these had an Ag core surrounded by an Au shell (so the opposite of the synthetic particles, which allowed clear differentiation of the original versus the biogenically produced NPs). The co-exposure to the two metals in different forms led to different accumulation patterns compared to the single metal exposure set ups, substantiating the importance of testing toxicity of chemical mixtures. Finally, the accumulated total Ag concentrations were not statistically different in any case, regardless of the Ag form exposed. This study provided clear evidence that assessment of the uptake of metal NPs is conservatively covered by the assessment of the uptake of their ionic counterpart.

Credit author statement

Baccaro M.: Conceptualization, Methodology, Investigation, Formal analysis, Data curation, Writing – original draft, Visualization. **Montaño M. D.**: Investigation, Writing – review & editing. **Cui X.**: Investigation, Writing – review & editing. **Mackevica A.**: Investigation, **Lynch I.**: Resources, Writing – review & editing. **von der Kammer F.**: Resources, Writing – review & editing. **Lodge R. W.**: Investigation, Writing – review & editing. **Khlobystov A. N.**: Resources, Writing – review & editing. **van den Brink N. W.**: Conceptualization, Methodology, Writing – review & editing, Supervision.

Declaration of competing interest

The authors declare that they have no known competing financial interests or personal relationships that could have appeared to influence the work reported in this paper.

Acknowledgments

This research was funded by the EU H2020 project NanoFASE (Nanomaterial Fate and Speciation in the Environment; grant no. 646002).

Appendix A. Supplementary data

Supplementary data to this article can be found online at https://doi.org/10.1016/j.chemosphere.2022.134909.

References

Akter, M., Sikder, M.T., Rahman, M.M., Ullah, A., Hossain, K.F.B., Banik, S., Hosokawa, T., Saito, T., Kurasaki, M., 2018. A systematic review on silver nanoparticles-induced cytotoxicity: physicochemical properties and perspectives. J. Adv. Res. 9, 1–16.

Alivio, T.E.G., Fleer, N.A., Singh, J., Nadadur, G., Feng, M., Banerjee, S., Sharma, V.K., 2018. Stabilization of Ag-Au bimetallic nanocrystals in aquatic environments mediated by dissolved organic matter: a mechanistic perspective. Environ. Sci. Technol. 52, 7269–7278.

Ardestani, M.M., van Straalen, N.M., van Gestel, C.A., 2015. Biotic ligand modeling approach: synthesis of the effect of major cations on the toxicity of metals to soil and aquatic organisms. Environ. Toxicol. Chem. 34, 2194–2204.

Arslan, Z., Ates, M., McDuffy, W., Agachan, M.S., Farah, I.O., Yu, W.W., Bednar, A.J., 2011. Probing metabolic stability of CdSe nanoparticles: alkaline extraction of free cadmium from liver and kidney samples of rats exposed to CdSe nanoparticles. J. Hazard Mater. 192, 192–199.

Baccaro, M., Undas, A.K., de Vriendt, J., van den Berg, J.H.J., Peters, R.J.B., van den Brink, N.W., 2018. Ageing, dissolution and biogenic formation of nanoparticles: how do these factors affect the uptake kinetics of silver nanoparticles in earthworms? Environ. Sci.: Nano 5, 1107–1116.

Bakircioglu, D., Kurtulus, Y.B., İbar, H., 2011. Comparison of extraction procedures for assessing soil metal bioavailability of to wheat grains. Clean 39, 728–734.

Bollyn, J., Willaert, B., Kerre, B., Moens, C., Arijs, K., Mertens, J., Leverett, D., Oorts, K., Smolders, E., 2018. Transformation-dissolution reactions partially explain adverse effects of metallic silver nanoparticles to soil nitrification in different soils. Environ. Toxicol. Chem. 37, 2123–2131.

Bourdineaud, J.P., Stambuk, A., Srut, M., Radic Brkanac, S., Ivankovic, D., Lisjak, D., Sauerborn Klobucar, R., Dragun, Z., Bacic, N., Klobucar, G.I.V., 2019. Gold and silver nanoparticles effects to the earthworm Eisenia fetida - the importance of tissue over soil concentrations. Drug Chem. Toxicol. 1–18.

Chang, Y.T., Hseu, Z.Y., Zehetner, F., 2014. Evaluation of phytoavailability of heavy metals to Chinese cabbage (Brassica chinensis L.) in rural soils. TheScientificWorldJOURNAL 309396, 2014.

Cornelis, G., Hund-Rinke, K., Kuhlbusch, T., van den Brink, N., Nickel, C., 2014. Fate and bioavailability of engineered nanoparticles in soils: a review. Crit. Rev. Environ. Sci. Technol. 44, 2720–2764.

Diez-Ortiz, M., Lahive, E., Kille, P., Powell, K., Morgan, A.J., Jurkschat, K., Van Gestel, C. A., Mosselmans, J.F.W., Svendsen, C., Spurgeon, D.J., 2015. Uptake routes and toxicokinetics of silver nanoparticles and silver ions in the earthworm Lumbricus rubellus. Environ. Toxicol. Chem. 34, 2263–2270.

Dong, L., Zhou, X., Hu, L., Yin, Y., Liu, J., 2018. Simultaneous size characterization and mass quantification of the in vivo core-biocorona structure and dissolved species of silver nanoparticles. J. Environ. Sci. 63, 227–235.

Ernst, W.H.O., 1996. Bioavailability of heavy metals and decontamination of soils by plants. Appl. Geochem. 11, 163–167.

Garcia-Alvarez, R., Hadjidemetriou, M., Sanchez-Iglesias, A., Liz-Marzan, L.M., Kostarelos, K., 2018. In vivo formation of protein corona on gold nanoparticles. The effect of their size and shape. Nanoscale 10, 1256–1264.

Gray, E.P., Coleman, J.G., Bednar, A.J., Kennedy, A.J., Ranville, J.F., Higgins, C.P., 2013. Extraction and analysis of silver and gold nanoparticles from biological tissues using single particle inductively coupled plasma mass spectrometry. Environ. Sci. Technol. 47, 14315–14323.

Hayashi, Y., Miclaus, T., Scavenius, C., Kwiatkowska, K., Sobota, A., Engelmann, P., Scott-Fordsmand, J.J., Enghild, J.J., Sutherland, D.S., 2013. Species differences take shape at nanoparticles: protein corona made of the native repertoire assists cellular interaction. Environ. Sci. Technol. 47, 14367–14375.

Kampe, S., Kaegi, R., Schlich, K., Wasmuth, C., Hollert, H., Schlechtriem, C., 2018. Silver nanoparticles in sewage sludge: bioavailability of sulfidized silver to the terrestrial isopod Porcellio scaber. Environ. Toxicol. Chem. 37, 1606–1613.

Kumar, S., Gandhi, K., Kumar, R., 2007. Modeling of formation of gold nanoparticles by citrate method. Ind. Eng. Chem. Res. 46, 3128–3136.

Lanno, R., Wells, J., Conder, J., Bradham, K., Basta, N., 2004. The bioavailability of chemicals in soil for earthworms. Ecotoxicol. Environ. Saf. 57, 39–47.

Laycock, A., Romero-Freire, A., Najorka, J., Svendsen, C., van Gestel, C.A.M., Rehkamper, M., 2017. Novel multi-isotope tracer approach to test ZnO nanoparticle and soluble Zn bioavailability in joint soil exposures. Environ. Sci. Technol. 51, 12756–12763.

Lo, I.M., Yang, X., 1999. EDTA extraction of heavy metals from different soil fractions and synthetic soils. Water Air Soil Pollut. 109, 219–236.

Loeschner, K., Brabrand, M.S., Sloth, J.J., Larsen, E.H., 2014. Use of alkaline or enzymatic sample pretreatment prior to characterization of gold nanoparticles in animal tissue by single-particle ICPMS. Anal. Bioanal. Chem. 406, 3845–3851.

Lundqvist, M., Stigler, J., Elia, G., Lynch, I., Cedervall, T., Dawson, K.A., 2008. Nanoparticle size and surface properties determine the protein corona with possible implications for biological impacts. Proc. Natl. Acad. Sci. U. S. A 105, 14265–14270.

Merrifield, R.C., Stephan, C., Lead, J., 2017. Determining the concentration dependent transformations of Ag nanoparticles in complex media: using SP-ICP-ms and Au@Ag core-shell nanoparticles as tracers. Environ. Sci. Technol. 51, 3206–3213.

Miclaus, T., Beer, C., Chevallier, J., Scavenius, C., Bochenkov, V.E., Enghild, J.J., Sutherland, D.S., 2016. Dynamic protein coronas revealed as a modulator of silver nanoparticle sulphidation in vitro. Nat. Commun. 7, 11770.

Mohsin, M., Jawad, M., Yameen, M.A., Waseem, A., Shah, S.H., Shaikh, A.J., 2020. An insight into the coating behavior of bimetallic silver and gold core-shell nanoparticles. Plasmonics 15.

Mondal, S., Roy, N., Laskar, R.A., Sk, I., Basu, S., Mandal, D., Begum, N.A., 2011. Biogenic synthesis of Ag, Au and bimetallic Au/Ag alloy nanoparticles using aqueous extract of mahogany (Swietenia mahogani JACQ.) leaves. Colloids Surf. B Biointerfaces 82, 497–504.

Montano, M.D., Majestic, B.J., Jamting, A.K., Westerhoff, P., Ranville, J.F., 2016. Methods for the detection and characterization of silica colloids by microsecond spICP-MS. Anal. Chem. 88, 4733–4741.

Naasz, S., Weigel, S., Borovinskaya, O., Serva, A., Cascio, C., Undas, A.K., Simeone, F.C., Marvin, H.J.P., Peters, R.J.B., 2018. Multi-element analysis of single nanoparticles by ICP-MS using quadrupole and time-of-flight technologies. J. Anal. Atomic Spectrom. 33, 835–845.

Noventa, S., Hacker, C., Rowe, D., Elgy, C., Galloway, T., 2018. Dissolution and bandgap paradigms for predicting the toxicity of metal oxide nanoparticles in the marine environment: an in vivo study with oyster embryos. Nanotoxicology 12, 63–78.

Pace, H.E., Rogers, N.J., Jarolimek, C., Coleman, V.A., Higgins, C.P., Ranville, J.F., 2011. Determining transport efficiency for the purpose of counting and sizing nanoparticles via single particle inductively coupled plasma mass spectrometry. Anal. Chem. 83, 9361–9369.

Savoly, Z., Hracs, K., Pemmer, B., Streli, C., Zaray, G., Nagy, P.I., 2016. Uptake and toxicity of nano-ZnO in the plant-feeding nematode, Xiphinema vuittenezi: the role of dissolved zinc and nanoparticle-specific effects. Environ. Sci. Pollut. Res. Int. 23, 9669–9678.

Sharma, V.K., Sayes, C.M., Guo, B., Pillai, S., Parsons, J.G., Wang, C., Yan, B., Ma, X., 2019. Interactions between silver nanoparticles and other metal nanoparticles under environmentally relevant conditions: a review. Sci. Total Environ. 653, 1042–1051.

Tavares, D.S., Rodrigues, S.M., Cruz, N., Carvalho, C., Teixeira, T., Carvalho, L., Duarte, A.C., Trindade, T., Pereira, E., Romkens, P.F., 2015. Soil-pore water distribution of silver and gold engineered nanoparticles in undisturbed soils under unsaturated conditions. Chemosphere 136, 86–94.

Unrine, J.M., Hunyadi, S.E., Tsyusko, O.V., Rao, W., Shoults-Wilson, W.A., Bertsch, P.M., 2010. Evidence for bioavailability of Au nanoparticles from soil and biodistribution within earthworms (Eisenia fetida). Environ. Sci. Technol. 44, 8308–8313.

van den Brink, N.W., Jemec Kokalj, A., Silva, P.V., Lahive, E., Norrfors, K., Baccaro, M., Khodaparast, Z., Loureiro, S., Drobne, D., Cornelis, G., Lofts, S., Handy, R.D., Svendsen, C., Spurgeon, D., van Gestel, C.A.M., 2019. Tools and rules for modelling uptake and bioaccumulation of nanomaterials in invertebrate organisms. Environ. Sci.: Nano.

Vijver, M.G., Vink, J.P., Miermans, C.J., van Gestel, C.A., 2003. Oral sealing using glue: a new method to distinguish between intestinal and dermal uptake of metals in earthworms. Soil Biol. Biochem. 35, 125–132.